

# Protein kinase C $\beta$ deficiency attenuates obesity syndrome of *ob/ob* mice by promoting white adipose tissue remodeling

Wei Huang,\* Rishipal R. Bansode,\* Naresh C. Bal,<sup>†</sup> Madhu Mehta,<sup>§</sup> and Kamal D. Mehta<sup>1,\*</sup>

Department of Molecular & Cellular Biochemistry, Dorothy M. Davis Heart & Lung Research Institute,\* Department of Physiology,<sup>†</sup> and the Department of Medicine,<sup>§</sup> The Ohio State University College of Medicine, 1645 Neil Avenue, Columbus, OH 43210

**Abstract** To explore the role of leptin in PKC $\beta$  action and to determine the protective potential of PKC $\beta$  deficiency on profound obesity, double knockout (DBKO) mice lacking PKC $\beta$  and *ob* genes were created, and key parameters of metabolism and body composition were studied. DBKO mice had similar caloric intake as *ob/ob* mice but showed significantly reduced body fat content, improved glucose metabolism, and elevated body temperature. DBKO mice were resistant to high-fat diet-induced obesity. Moreover, PKC $\beta$  deficiency increased  $\beta$ -adrenergic signaling by inducing expression of  $\beta$ 1- and  $\beta$ 3-adrenergic receptors ( $\beta$ -ARs) in white adipose tissue (WAT) of *ob/ob* mice. Accordingly, p38<sup>MAPK</sup> activation and expression of PGC-1 $\alpha$  and UCP-1 were increased in WAT of DBKO mice. Consistent with results of in vivo studies, inhibition of PKC $\beta$  in WAT explants from *ob/ob* mice also increased expression of above  $\beta$ -ARs. In contrast, induction of PGC-1 $\alpha$  and UCP-1 expression in brown adipose tissue of DBKO mice was not accompanied by changes in the expression of these  $\beta$ -ARs. Collectively, these findings suggest that PKC $\beta$  deficiency may prevent genetic obesity, in part, by remodeling the catabolic function of adipose tissues through  $\beta$ -ARs dependent and independent mechanisms.—Huang, W., R. R. Bansode, N. Bal, M. Mehta, and K. D. Mehta. Protein kinase C $\beta$  deficiency attenuates obesity syndrome of *ob/ob* mice by promoting white adipose tissue remodeling. *J. Lipid Res.* 2012. 53: 368–378.

**Supplementary key words** protein kinase C $\beta$  • adipose tissue remodeling •  $\beta$ -adrenergic receptors • thermogenesis

Leptin is an adipocyte-derived hormone that is required for normal energy homeostasis (1–3). It plays a key role in the control of body weight by suppressing food intake through actions on hypothalamic receptors and by increasing energy expenditure via activation of sympathetic activity and brown adipose tissue (BAT) thermogenesis. This is

best illustrated by loss of function mutations in genes encoding leptin or the leptin receptor, which result in severe obesity in rodents and humans. Leptin is also known to play a dual role in glucose metabolism and insulin signaling, acting as an insulin sensitizer and as an antagonist. In vivo, leptin has been reported to enhance insulin action in inhibiting hepatic glucose output while antagonizing insulin action on the expression of metabolic genes (4). The insulin and leptin signaling pathways are known to share downstream targets such as Janus kinase-2, insulin receptor substrates, phosphatidylinositol 3-kinase, protein kinase B, mitogen-activated protein kinase, and protein kinase C (PKC). Recent data provide evidence that PKC is activated by leptin via increasing calcium concentration and stimulating inositol triphosphate (IP-3) production (5). PKC-dependent phosphorylation of Ser-318 in insulin receptor substrate-1 has been implicated in mediating the inhibitory signal of leptin on the insulin-signaling cascade (6). Several other interactions in different physiological systems have been described between PKC and leptin (7–10).

PKCs comprise a large family of serine/threonine protein kinases that plays a key role in signal transduction and regulation of gene expression (11–14). Twelve distinct members have been discovered in mammalian cells, and these have been subdivided into three distinct subfamilies as follows: conventional PKCs ( $\alpha$ ,  $\beta$ I,  $\beta$ II, and  $\gamma$ ), novel PKCs ( $\delta$ ,  $\epsilon$ ,  $\nu$ , and  $\theta$ ), and atypical PKCs ( $\xi$  and  $\iota/\lambda$ ). These PKC isoforms are unique not only with respect to their primary structures but also in their expression patterns, subcellular localization, in vitro activation, and responsiveness to

Abbreviations:  $\beta$ -AR, beta-adrenergic receptor; BAT, brown adipose tissue; DBKO, *ob/ob* mice deficient in PKC $\beta$ ; HFD, high-fat diet; *ob/ob*, leptin-deficient mice; p38MAPK, stress-activated mitogen-activated protein kinase; PGC-1 $\alpha$ , peroxisome-proliferator-activated receptor  $\gamma$  coactivator-1 $\alpha$ ; PKC, protein kinase C; PKC $\beta$ , protein kinase C $\beta$ ; PKC $\beta$ <sup>-/-</sup>, PKC $\beta$ -deficient mice; p38<sup>MAPK</sup>, stress-regulated mitogen-activated protein kinase; SIRT, sirtuin; TG, triglyceride; UCP-1, uncoupling protein-1; WAT, white adipose tissue; iWAT, inguinal WAT; eWAT, epididymal WAT.

<sup>1</sup>To whom correspondence should be addressed.  
e-mail: Mehta.80@osu.edu

This work was supported by National Institutes of Health grant HL-79091 (K.D.M.). Its contents are solely the responsibility of the authors and do not necessarily represent the official views of the National Institutes of Health.

Manuscript received 16 August 2011 and in revised form 29 December 2011.

Published, JLR Papers in Press, December 30, 2011

DOI 10.1194/jlr.M019687

extracellular signals. Most importantly, these isoforms show differences in cofactor dependence and responsiveness to calcium and phospholipid metabolites. Conventional PKCs bind to and are activated by sn-1,2-diacylglycerol, which increases the specificity of the enzyme for phosphatidylserine and its affinity for calcium. Novel PKCs are also activated by DAG and require phosphatidylserine as a cofactor but have lost the requirement for calcium. Atypical PKCs do not respond to DAG or calcium but apparently still require phosphatidylserine as a cofactor. Recent studies have shown that DAG-PKC signaling is activated in diabetic conditions, and the induction appears to be restricted to a few “diabetic-related” isoforms (15, 16). PKC $\beta$  is one isoform that has been most directly linked to important aspects of hyperglycemia in vivo and in vitro. PKC $\beta$  was also one of the earliest isoforms recognized in insulin signaling and appears to play dual roles in insulin signaling pathways (17–22). PKC $\beta$  does not appear to regulate glucose-induced insulin secretion in vivo (23), even though it has been reported to undergo translocation to the plasma membrane subsequent to stimulation by glucose in primary islet cells (24). We recently showed that PKC $\beta$  is markedly elevated in white adipose tissue (WAT) of leptin-deficient (*ob/ob*) mice and is significantly induced by intake of high-fat diet (HFD) (25, 26). We also assessed the impact of PKC $\beta$  deficiency on glucose and lipid homeostasis in vivo and found that deficiency of PKC $\beta$  signaling resulted in adipose atrophy, hypoleptinemia, hyperphagia, and altered expression of genes involved in energy homeostasis in the adipose tissue. The lean phenotype of PKC $\beta$ <sup>-/-</sup> mice was associated with reduced serum leptin and compensatory increased food intake (26). Furthermore, adiposity is not increased when PKC $\beta$ -deficient (PKC $\beta$ <sup>-/-</sup>) mice are challenged with a HFD. These studies identified the PKC $\beta$  signaling pathway as a novel modulator of adipose tissue homeostasis.

Unlike PKC $\beta$ <sup>-/-</sup> mice, *ob/ob* mice exhibit marked obesity, hyperphagia, insulin resistance, hypothermia, and increased food efficiency. To explore the protective potential of PKC $\beta$  deficiency on profound obesity and to better understand the regulatory pathways that govern energy metabolism, we examined the effects of PKC $\beta$  gene disruption in genetically obese *ob/ob* mice on diverse elements of energy balance, focusing particularly on the  $\beta$ -AR signaling. We report that deletion of PKC $\beta$  in *ob/ob* mice (DBKO) decreases food efficiency through increasing energy expenditure and thermogenesis and through enhanced insulin sensitivity, thus improving the energy balance of *ob/ob* mice. A significant component of the effect of PKC $\beta$  deficiency on energy expenditure is independent of leptin and involves signaling through  $\beta$ -ARs in WAT. In fact, enhanced  $\beta$ -adrenergic signaling may account for hypoleptinemia in PKC $\beta$ <sup>-/-</sup> mice.

## MATERIALS AND METHODS

### Animals and diet

A double knockout mouse simultaneously lacking the leptin and PKC $\beta$  genes was generated by intercrossing male *ob/ob*<sup>+/-</sup> mice with female PKC $\beta$ <sup>-/-</sup> mice on a C57BL/6J background

(Jackson Laboratories, Bar Harbor, ME) to generate *ob*<sup>+/-</sup> x PKC $\beta$ <sup>-/-</sup>. These leptin heterozygous and PKC $\beta$  homozygous mice were used to generate double knockout *ob/ob* x PKC $\beta$ <sup>-/-</sup> mice. Genotyping for *ob/ob* and PKC $\beta$  were performed as previously described (25). Unless indicated, all experiments were performed on male animals.

Male mice were weaned at 21 days of age, genotyped, and maintained at a room temperature of 22 ± 2°C on a 12:12 light-dark cycle with a relative humidity of 50%. Animals had free access to water and were fed ad libitum. Body weight and food intake were registered weekly. Body temperature was assessed by measuring rectal temperature using a rectal thermometer.

Seven- to eight-week-old *ob/ob* and DBKO mice were fed ad libitum for the indicated period continuously either on a HFD (D12492; Research Diets, New Brunswick, NJ) in which 60% of the total calories were derived from fat (soybean oil and lard) or a standard diet containing 17% kcal from fat (7912 rodent chow; Harlan Laboratories, Inc., Indianapolis, IN) (25). All procedures on mice followed guidelines established by the Ohio State University College of Medicine Animal Care Committee. Unless indicated, all experiments were performed on mice starved for approximately 16 h.

### Blood and tissue collection

Eighteen-week-old mice were fasted for 6 h and euthanized by CO<sub>2</sub> inhalation. Blood samples were obtained by submandibular bleeding, and plasma or sera were collected after centrifugation (4°C) at 12,000 rpm for 15 min and stored at -20°C. Epididymal, inguinal, and retroperitoneal white adipose tissues, together with brown fat from the interscapular depot, and livers were carefully excised. Tissue samples were weighed and then immediately frozen in liquid nitrogen. For morphological assessment, parts of adipose tissue was fixed in 4% buffered formaldehyde overnight and then dehydrated in graded ethanols and embedded in paraffin. Sections (10  $\mu$ m) were cut and mounted on slides and stained with hematoxylin and eosin or UCP-1 antibody (1:500)-HRP according to standard protocols. Plasma concentrations of triglycerides, total cholesterol, and serum-free fatty acids were measured by enzymatic methods using commercially available kits. Serum insulin and adiponectin were determined by ELISA.

### Glucose tolerance test and insulin tolerance test

A glucose tolerance test and insulin tolerance test were performed on fasted (16 h) mice. Mice were weighed and injected intraperitoneally with glucose (1.5 mg/kg body weight) or insulin (0.8 U/kg body weight). Blood samples were collected via tail bleeds, and glucose concentrations were measured before and 15, 30, 60, 90, and 120 min after the challenge. Glucose was determined by glucometer.

### Oxygen consumption measurements

Oxygen consumption, CO<sub>2</sub> production, and spontaneous physical movement were measured simultaneously over 24 h for each mouse using a computer-controlled, open-circuit Oxymax/CLAMS System (Columbus Instruments, Columbus, OH). Each mouse was measured individually in a resting state at 22°C in the presence of food and water.

### Western blot studies

Tissues were homogenized in buffer containing 20 mM Tris, 50 mM NaCl, 250 mM sucrose, 1% Triton X-100, and phosphatase and protease inhibitors cocktail, and protein content was measured as described earlier (25). Equal amounts of protein were run in 12% SDS-PAGE, transferred to nitrocellulose membranes, and blocked in Tris-buffered saline with Tween 20 containing 5%

nonfat dry milk or BSA for 1 h at room temperature. Blots were incubated overnight at 4°C with primary antibodies against UCP-1 (Abcam, Cambridge, MA) at 1:2,000; or P-p38MAPK (Cell Signaling Technology, Inc., Boston, MA) at 1:1,000, or p38MAPK (Santa Cruz Biotechnology, Santa Cruz, CA) at 1:2,000. The antigen-antibody complexes were visualized using peroxidase-conjugated anti-rabbit antibodies (1:5,000) and the enhanced chemiluminescence ECL detection system (Life Technologies, Grand Island, NY). All assays were performed in duplicate.

### In vitro analysis of isolated inguinal WAT (explants)

Inguinal, epididymal WAT, or interscapular BAT were surgically removed from *ob/ob* and DBKO mice (n = 3 per group). Freshly dissected fat pads were minced to a size of 2–3 mm<sup>3</sup> for iWAT and 1–2 mm<sup>3</sup> for BAT on an ice-cold Petri dish containing Krebs-Ringer HEPES buffer (5 mM D-glucose, 2% BSA, 135 mM NaCl, 2.2 mM CaCl<sub>2</sub>, 1.25 mM MgSO<sub>4</sub>, 0.45 mM KH<sub>2</sub>PO<sub>4</sub>, 2.17 mM Na<sub>2</sub>HPO<sub>4</sub>, and 10 mM HEPES) and then rinsed twice with Krebs-Ringer HEPES buffer and once with DMEM containing 10% BSA. Samples were passed through a 200-μm mesh. The tissue explants were transferred to 6-well plate with an equal amount of the tissue in each well. The explants were allowed to stabilize in DMEM medium for 1 h before the treatment. All procedures were performed under sterile conditions. LY333,531 from Alexis Biochemicals was added to each well as indicated for 16 h. Explants were transferred to a 2 ml tube and rinsed with PBS twice before being snap-frozen in liquid nitrogen for later analysis of gene expression.

### Gene expression

Total RNA was extracted from iWAT and BAT samples by homogenization using TRIzol reagent. Samples were treated with a DNA-free kit (Life Technologies, Grand Island, NY). For first-strand cDNA synthesis, constant amounts of 2 μg of total RNA were reverse transcribed in a 20 μl final volume using random

hexamers as primers and 50 units of MultiScribe™ Reverse Transcriptase (High-capacity cDNA Reverse Transcription Kit, Life Technologies, Grand Island, NY) (25, 26). The transcript levels for indicated genes were quantified as described earlier. Relative mRNA expression was expressed as fold expression over the control mice. All samples were run in triplicate, and the average values were calculated.

### Statistical analysis

The results are shown as means ± SEM. All statistical analysis was performed by Student *t*-test or ANOVA in Excel; *P* < 0.05 was considered significant.

## RESULTS

### Ablation of PKCβ reduces the positive energy balance of *ob/ob* mice

To explore the effects of PKCβ deficiency on *ob/ob* phenotype, we intercrossed *ob*<sup>-/+</sup> with PKCβ<sup>-/-</sup> mice to generate DBKO mice. Body weight and fat content were compared between *ob/ob* and DBKO mice. Compared with the *ob/ob* mice of the same age, DBKO mice have lower body weight (Fig. 1A–C). Noteworthy differences in body weights were apparent by as early as 7 weeks of age and became even more pronounced with aging. At 18 weeks of age, weight was reduced by 34% in female mice and by 29% in male mice. It was accompanied by significantly reduced inguinal and retroperitoneal white fat depots per body weight as compared with *ob/ob* mice in male (Fig. 1D, E) and female mice (results not shown). The wet weight of inguinal white adipose tissue (iWAT) was reduced by ~41% in DBKO in comparison to *ob/ob* mice. The weights

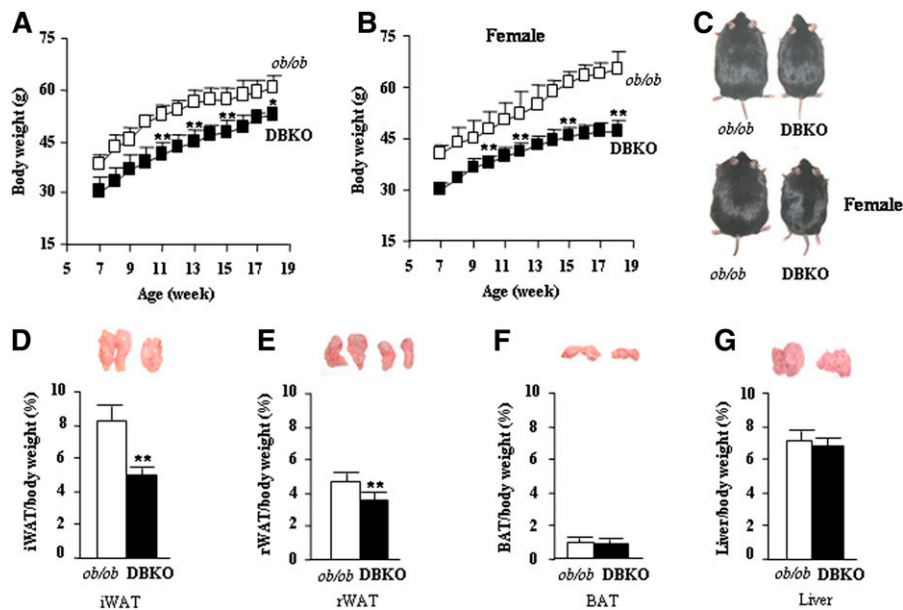


**Fig. 1.** Physical appearance, growth curves, adipose stores and livers of *ob/ob* and DBKO mice. At 7 week of age, male (A) and female (B) mice fed standard chow diet were weighed weekly. C: Gross representative images of 18-week-old male and female *ob/ob* and DBKO mice on a C57BL/6J background. D–G: Representative pictures and weights of iWAT, rWAT, BAT, and liver for 18-week-old male mice fed chow diet. Values represent the means ± SE of *ob/ob* and DBKO mice (n = 12). \**P* < 0.05; \*\**P* < 0.01.

of other tissues, including liver and brown adipose tissue (BAT), were similar between genotypes (Fig. 1F, G). Histology of inguinal WAT (iWAT) of DBKO mice revealed unilocular white adipocytes that were smaller than those in *ob/ob* mice and abundant, more densely stained and much smaller cells, many with a multilocular appearance (Fig. 2A).

Brown fat is critical for adaptive thermogenesis in mice. DBKO mice also tend to show reduced absolute weight of BAT compared with *ob/ob* mice, but the difference did not reach statistical significance when body weight was considered (Fig. 1F). Compared with the control *ob/ob* mice, the size of brown adipocytes was much smaller in the DBKO mice (Fig. 2A). Furthermore, brown adipocytes showed small and multilocular lipid droplets in DBKO mice, whereas *ob/ob* mice exhibited large and unilocular lipid droplets, suggesting higher thermogenic activity in DBKO mice leading to reduction in fat accumulation.

*ob/ob* mice have massively enlarged livers that are engorged with lipid (Fig. 1G). Histological sections of *ob/ob* liver showed large lipid-filled vacuoles, whereas those of DBKO mice showed significantly smaller lipid-filled vacuoles (Fig. 2A). Consistent with histological examination, hepatic TG content was greatly reduced in DBKO mice (Fig. 2B, C). In addition to a reduced amount of TG in the liver, the amount of TG in the skeletal muscle of DBKO mice was also significantly reduced (Fig. 2B, C). Therefore, the reduced TG levels in adipose tissue were not due to alternative lipid storage in other tissues, such as liver and muscle. It remains to be seen whether reduction in TG biosynthesis contributes to the overall reduction in the body's TG contents.

Adiposity is influenced by the rate of food consumption and the rate at which energy is expended metabolically. To determine whether change in food intake and/or energy expenditure was responsible for decreased obesity of DBKO mice relative to *ob/ob* mice, we compared their rates of food intake and oxygen consumption. With or without normalization for body weight, Fig. 3A and 3B show that male DBKO mice consumed a similar level of food as male *ob/ob* mice; this rate of food intake was also seen with female mice (results not shown), suggesting that the decrease in food intake cannot account for the failure of DBKO mice to gain weight. Interestingly, basal oxygen consumption at night was significantly higher in male DBKO mice than in male *ob/ob* mice (Fig. 3C, D). Thus, increased metabolic rate may help to normalize energy balance in DBKO mice. We cannot rule out whether the differences in body weight contribute to increased oxygen consumption of DBKO mice compared with *ob/ob* mice (27, 28). The increased oxygen consumption could also be due in part to the maintenance of a higher body temperature of DBKO mice (Fig. 3E). These data strongly suggest that PKC $\beta$  deficiency may increase energy expenditure in *ob/ob* mice.

#### DBKO mice exhibit improved insulin sensitivity

Changes in adiposity are often associated with alterations in glucose and insulin homeostasis. The *ob/ob* mice develop a form of diabetes similar to human type-2 diabetes, a condition commonly associated with obesity. To evaluate the effect of PKC $\beta$  deficiency on glucose metabolism in chow-fed mice, we first evaluated plasma glucose and

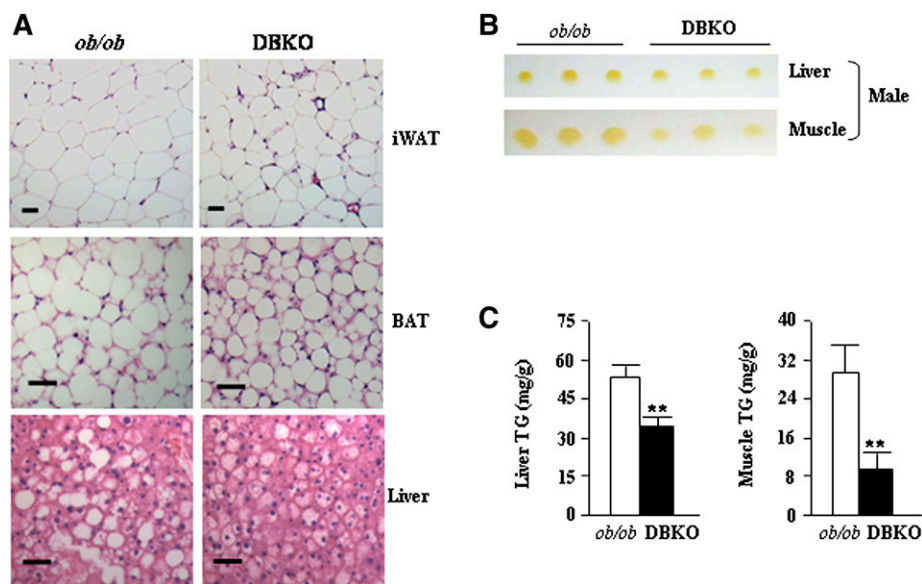


**Fig. 2.** Histological and biochemical changes in liver, adipose, and muscle TG content of male *ob/ob* and DBKO mice. A: Hematoxylin and eosin (H+E) staining of iWAT, interscapular BAT, and liver from male *ob/ob* and DBKO mice. Results are representative of  $n = 6$  in each group. Bar, 5  $\mu$ M. B: Thin-layer chromatography of total lipid extracts from liver and muscle of both genotypes is also shown. Each lane represents lipids from the liver and muscle of three mice of each genotype. C: Relative amounts of TG contents in the liver and muscle of male mice of both genotypes (fasted 16 h). Each value represents the means  $\pm$  SE ( $n = 6$  per genotype). \*\* $P < 0.01$ .

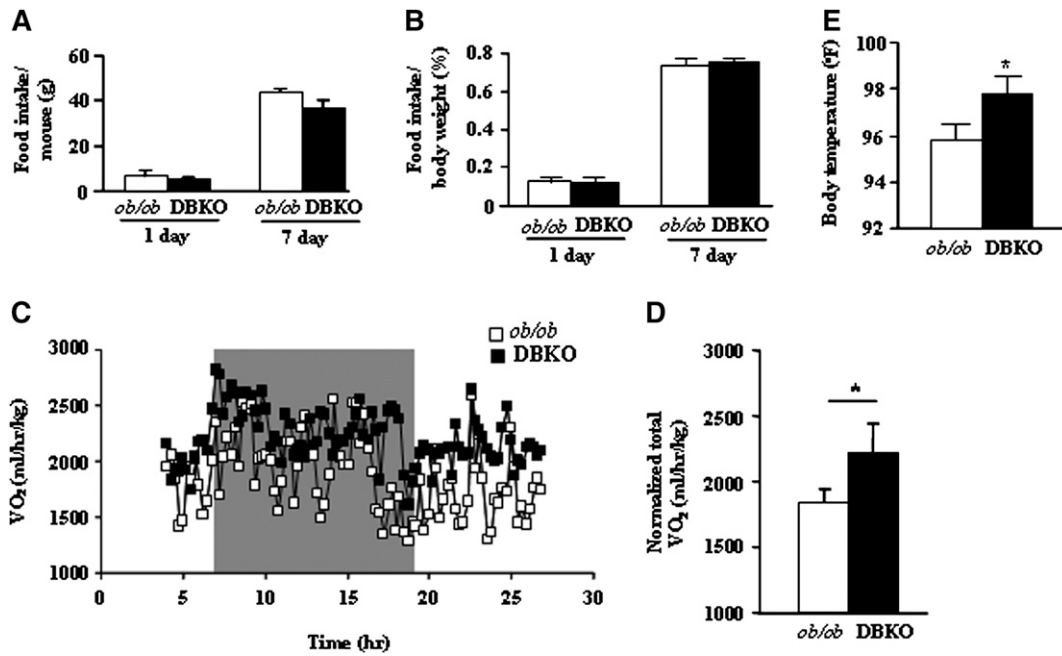


**Fig. 3.** Food intake, energy expenditure, and body temperature of male *ob/ob* and DBKO mice. A, B: Average daily food consumption. Food intake was determined by measuring 1 day or 7 day intake of chow diet by 12 week-old male mice;  $n = 12$  for each genotype. C and D: Metabolic rate and oxygen consumption of 12- to 14-week-old male mice on chow diet ( $n = 5$  each genotype) as measured by indirect calorimetry. Mice were monitored for 24 h continuously, from 10:00 AM to 10:00 AM the next day. To allow for acclimation, data from the initial 5 h are omitted. E: Average rectal temperatures for both genotypes. All values are given as means  $\pm$  SE. \* $P < 0.05$  compared with *ob/ob* mice.

insulin levels between genotypes. Both were significantly lower in fasted DBKO mice compared with those in *ob/ob* mice (Fig. 4A). Moreover, glucose to insulin ratios in DBKO mice was also significantly elevated (Fig. 4A), indicating improved insulin sensitivity. Meanwhile, DBKO mice showed a significant decrease in plasma glucose compared with *ob/ob* mice after intraperitoneal injection of glucose or insulin, indicating improved glucose metabolism by PKC $\beta$  deficiency in *ob/ob* mice (Fig. 4B). In agreement with the above findings, DBKO mice showed a significant increase in the whole body glucose uptake, further supporting improved glucose metabolism (Huang et al., unpublished results).

#### PKC $\beta$ deficiency protects *ob/ob* mice from HFD-induced obesity

We also compared responses of *ob/ob* and DBKO mice under conditions of severe dietary stress. Both genotypes were fed HFD beginning at 8 weeks of age. Body weights and food intake were monitored weekly, and at the end we examined weights of adipose tissues and various metabolic parameters. A significant increase in *ob/ob* mice body weights were evident even after 2 weeks on HFD, and this trend continued throughout the dietary protocol (Fig. 5A, B). DBKO mice fed HFD gained less weight than *ob/ob* mice and exhibited an obese-resistant phenotype (Fig. 5B).

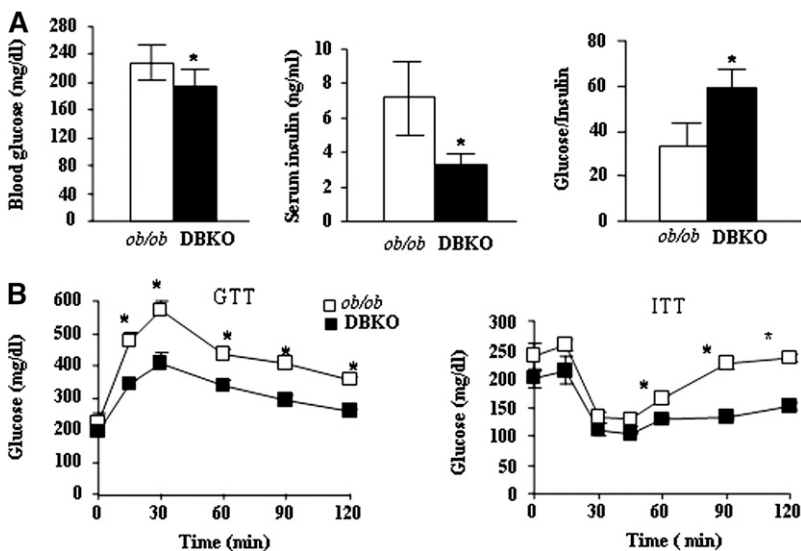


**Fig. 4.** Increase in vivo insulin sensitivity of DBKO mice compared with *ob/ob* mice. A: Blood glucose and serum insulin levels were measured in 12-week-old male *ob/ob* and DBKO mice and then glucose to insulin ratio was calculated accordingly. Data are expressed as means  $\pm$  SE ( $n = 6$ ). B: Changes in glucose levels in glucose-tolerance tests (GTT) and insulin-tolerance tests (ITT). Male mice fasted for approximately 16 h were injected with a bolus of glucose (1.5 mg/kg body weight) or insulin (0.8 U/kg body weight), and blood glucose levels were analyzed with a glucometer. Data are expressed as mean  $\pm$  SE ( $n = 6$ ). \* $P < 0.05$ .

The difference in body weights between *ob/ob* and DBKO mice was further reflected by marked reduction in iWAT and rWAT mass in DBKO mice, indicating that these mice are strongly protected from HFD-induced obesity (Fig. 5C, D). Histological analysis of iWAT revealed smaller adipocytes than those from *ob/ob* mice fed HFD (Fig. 5C). The weights of DBKO BAT and livers were almost comparable between these genotypes (Fig. 5E, F). Liver tissue appearance in *ob/ob* male mice was more whitish in color than that in DBKO mice. Similarly, *ob/ob* mice had higher hepatic TG content than DBKO mice (Fig. 5G) and exhibit increased glucose/insulin ratio (Fig. 5H). It is again clear that the decreased body weight was not a result of reduced food intake of DBKO mice compared with *ob/ob* mice (Fig. 6). Indirect calorimetry measurements revealed a significant increase in oxygen consumption (Fig. 7A, B) in HFD-fed DBKO mice compared with *ob/ob* mice. In the DBKO mice, the increase in energy expenditure was more prominent at night when mice actively took food (Fig. 7A). The respiratory quotient was comparable in the *ob/ob* and DBKO mice (Fig. 7C, D), indicating similar utilization of carbohydrates and fat as energy sources.

#### PKC $\beta$ deficiency promotes upregulation of brown adipocyte function markers in WAT and BAT of *ob/ob* mice

To gain further insight into mechanisms underlying improved energy expenditure of DBKO mice, gene expression

levels of key molecules involved in the regulation of mitochondrial function and thermogenesis were analyzed. The elevated energy expenditure in DBKO mice led us to first study BAT, which is responsible for adaptive thermogenesis in response to diet or cold (29–31). Diet-induced thermogenesis reduces obesity in humans and animals (32, 33). Leptin deficiency is always associated with a reduction of PGC-1 $\alpha$  transcript levels, together with a tendency toward a decrease in sirtuin (SIRT)-1 transcript levels, without changes in expression levels of SIRT-3. On the contrary, DBKO mice showed a significant upregulation of PGC-1 $\alpha$ , UCP-1, SIRT-1, and SIRT-3, as compared with the *ob/ob* group (Fig. 8A). The protein expression of UCP-1 in BAT exhibited a pattern similar to that observed in the gene expression analyses for DBKO mice on chow or on the HFD diet (Fig. 8B, C).

A formalin-fixed, paraffin-embedded section from iWAT for UCP-1 protein stain appears to indicate a morphological change toward a BAT-like phenotype in DBKO (Fig. 8D). To determine the extent of shifting of the physiology and gene expression profiles of iWAT to BAT in DBKO mice, we checked expression levels of BAT-specific genes and several transcriptional regulators. Indeed, mRNA and protein levels of brown fat-specific gene UCP-1 were significantly elevated in the iWAT of DBKO mice compared with that of *ob/ob* mice (Fig. 8A, B). In addition, the mRNA level of PGC-1 $\alpha$  was also increased (Fig. 8A).

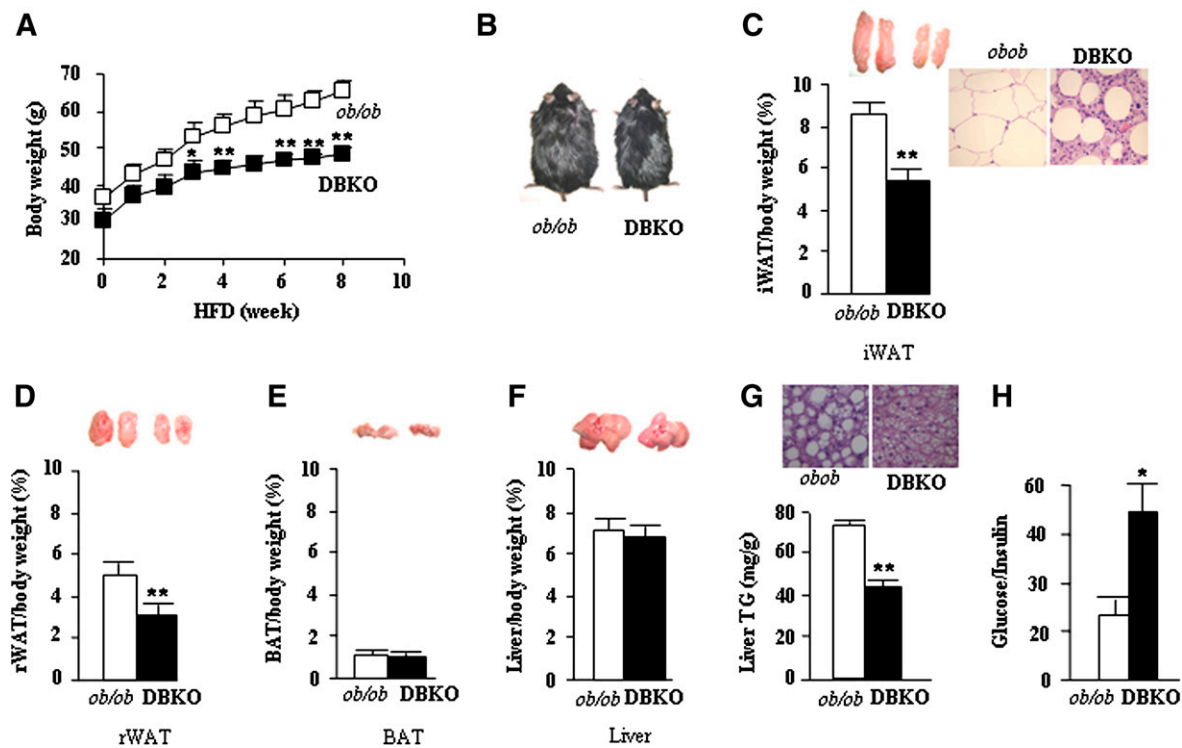


**Fig. 5.** DBKO mice are resistant to HFD-induced obesity. A: Growth curves of male mice fed HFD for the indicated period. Eight-week-old *ob/ob* and DBKO mice fed this diet were weighed weekly. Values represent mean  $\pm$  SE ( $n = 8$  of each genotype). B: Gross representative images of male *ob/ob* and DBKO mice before euthanization. C–F: Representative pictures and weights of iWAT, rWAT, BAT, and liver of HFD-fed male mice. G: Hematoxylin and eosin (H+E) staining and TG content of liver (magnification  $\times 20$ ) from *ob/ob* and DBKO mice. H: Glucose/insulin ratio. Values are the means  $\pm$  SE of *ob/ob* and DBKO mice ( $n = 6$ ). \* $P < 0.05$ ; \*\* $P < 0.01$ .

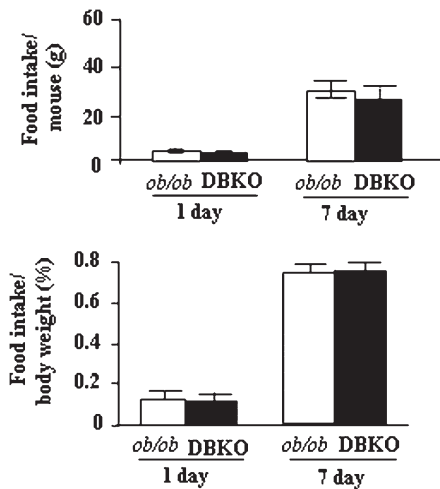


**Fig. 6.** Average daily food consumption. Food intake was determined by measuring 1 day or 7 day intake of HFD by 12-week-old male mice ( $n = 12$  for each genotype). Values represent the means  $\pm$  SE of *ob/ob* and DBKO mice.

### Increased expression of $\beta$ 3-adrenergic receptor and signaling in WAT, and not BAT, of DBKO mice

UCP-1 expression is regulated by sympathetic input through  $\beta$ -ARs- and cAMP-dependent mechanisms (34, 35). We therefore examined expression levels of all three  $\beta$ -ARs in adipose tissues of both genotypes. Expression levels of  $\beta$ 1- and  $\beta$ 3-ARs were elevated in WAT of DBKO mice compared with *ob/ob* mice, whereas expression levels of  $\beta$ 2-AR remained unchanged (Fig. 9A). In contrast, BAT of both genotypes revealed similar levels of  $\beta$ -ARs (results not shown).

To explore the potential relationship between PKC $\beta$  and  $\beta$ -AR expression, iWAT explants were prepared from *ob/ob* and DBKO mice. Treatment with a specific PKC $\beta$  inhibitor, LY333,531, increased expression of  $\beta$ 1- and  $\beta$ 3-ARs, but not  $\beta$ 2-AR, of *ob/ob* mice but not of DBKO mice (Fig. 9B). Also, explants from BAT of *ob/ob* or DBKO mice did not show alterations in the expression of  $\beta$ -ARs, which is consistent with the above in vivo observation (results not shown).

Consistent with an increased  $\beta$ -adrenergic signaling, greater p38<sup>MAPK</sup> phosphorylation was observed in iWAT of DBKO mice compared with *ob/ob* mice (Fig. 10A). Inhibition of p38<sup>MAPK</sup> by using a specific inhibitor, SB202,190, significantly reduced  $\beta$ 3-AR agonist (CL341,243)-induced PGC-1 $\alpha$  expression (Fig. 10B), suggesting the requirement of p38<sup>MAPK</sup> in the induction process.

## DISCUSSION

Our findings show that PKC $\beta$  deficiency in *ob/ob* mice produces an integrated series of molecular, cellular, and physiological responses that have a profound impact on energy expenditure without affecting the energy intake component of the energy balance equation. The net effect of these responses is a decrease in metabolic efficiency and a corresponding decrease in fat accretion in adipose tissue of DBKO mice compared with *ob/ob* mice. These results support the view that PKC $\beta$  plays an essential role in energy homeostasis by repressing metabolic genes involved in energy expenditure.

The substantial increase in energy expenditure induced by PKC $\beta$  deficiency in *ob/ob* mice is associated with elevated expression of UCP-1 in two distinct populations of

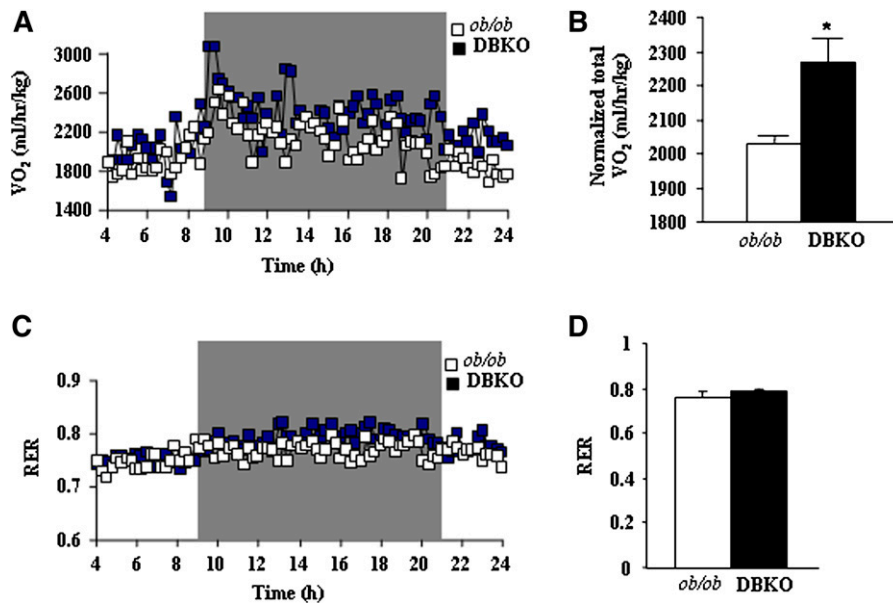


**Fig. 7.** Energy expenditure and body temperature of male *ob/ob* and DBKO mice fed HFD. A–C: Metabolic rate and oxygen consumption of 12- to 14-week-old mice on a chow diet ( $n = 5$  each genotype) as measured by indirect calorimetry. Mice were monitored for 24 h continuously, from 10:00 AM to 10:00 AM the next day. To allow for acclimation, data from the initial 3 h are omitted. All values are given as means  $\pm$  SE. \* $P < 0.05$  compared with *ob/ob* mice.

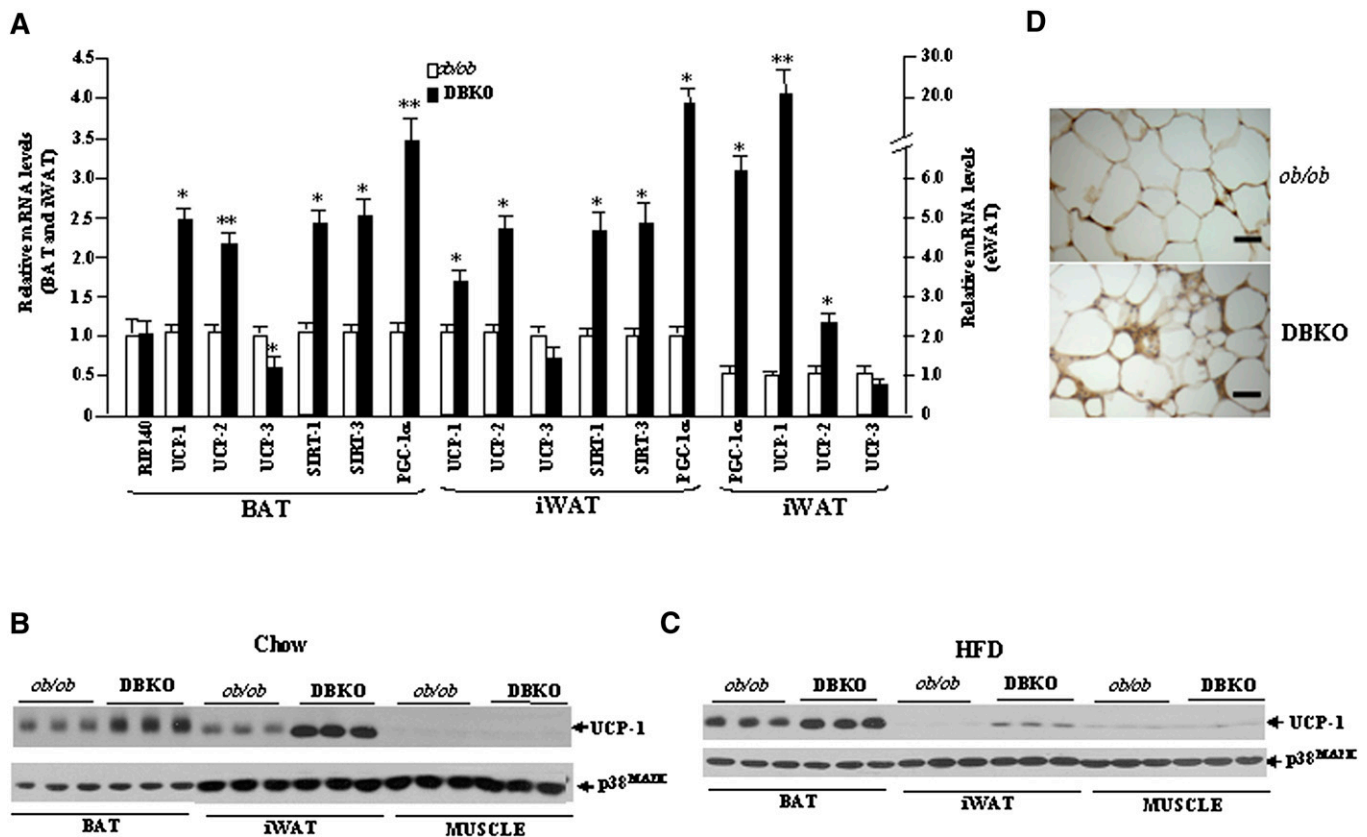


**Fig. 8.** Altered expression levels of crucial metabolic regulators and BAT-specific factors in DBKO mice compare with *ob/ob* mice. **A:** Bar graphs show mRNA levels of indicated genes normalized for the expression of  $\beta$ -actin in male mice fed HFD. The expression in WT mice was assumed to be 1. **B** and **C:** Levels of UCP-1 protein analyzed with Western blot in the BAT (0.5  $\mu$ g), iWAT (40  $\mu$ g), and muscle (40  $\mu$ g) from 12-week-old male *ob/ob* and DBKO mice fed chow or HFD for 8 weeks. Protein data were normalized for the expression of p38<sup>MAPK</sup>. **D:** UCP-1 staining of iWAT by immunohistochemistry. Brown stains indicate UCP-1 protein that appear in smaller adipocytes in iWAT of DBKO mice. Bar, 5  $\mu$ m. These figures are representative of three different experiments. Values given are means  $\pm$  SE. \* $P$  < 0.05; \*\* $P$  < 0.01 ( $n$  = 6 per group).

brown adipocytes. First, there was improvement in the function of brown adipocytes in BAT itself. On histological analysis, large unilocular lipid droplets were observed in BAT of *ob/ob* mice, whereas in DBKO mice the characteristic macroscopic, microscopic, and molecular features of BAT are partially restored. Second, expression of UCP-1 protein, which is normally restricted to brown adipocytes, is induced in what is usually regarded as WAT (iWAT) in DBKO mice. A similar response is seen in rats and mice after cold exposure or treatment with  $\beta$ 3-AR agonists (36–39). Moreover, considerable precedent exists to support the association between an increase in UCP-1-dependent energy expenditure and leanness in mouse models (40–43). For example, overexpression of UCP-1 in WAT and BAT using a transgene driven by the fat-specific aP2 promoter resulted in lower adiposity, as did the disruption of the Cidea protein, a mitochondrial component that was shown to suppress UCP-1 activity (42). The common finding in these studies is that the observed increase in cAMP signaling or  $\beta$ -AR sensitivity, which induced UCP-1 expression in WAT, produces a similar lean, obesity-resistant phenotype. This is accomplished by activation of p38<sup>MAPK</sup> signaling, which leads to the activation of transcription factors, such as ATF2 and CREB, and increased expression

and phosphorylation of the nuclear factor cofactor PGC-1 $\alpha$ . Our findings also support the view that a significant component of the mechanism engaged by PKC $\beta$ <sup>-/-</sup> mice to increase energy expenditure involves signaling through  $\beta$ -AR. Accordingly, p38<sup>MAPK</sup> activation and the expression of PGC-1 $\alpha$ , a key marker of brown fat cell function, were increased in WAT of DBKO mice. PGC-1 $\alpha$  is an important factor in mitochondrial function and energy homeostasis and controls several aspects of mitochondrial biogenesis. It plays an essential role in brown fat thermogenesis through activation of UCP-1 (44). In addition, increases in the expression of SIRT-1 and SIRT-3 genes can influence energy homeostasis in the adipose tissues of DBKO mice. SIRT-1 is known to positively act on the activation of metabolic genes through direct deacetylation of PGC-1 $\alpha$  (45, 46). Also, growing evidence supports a novel role for SIRT-3 in enhancing the expression of mitochondrial-related genes, participating in adaptive thermogenesis (47).

It is well known that PGC-1 $\alpha$  is intimately involved in adaptive thermogenesis via the induction of the mitochondrial inner membrane uncoupling protein UCP-1 (48), thereby providing one potential mechanism contributing to the lean phenotype of DBKO mice. In addition to transcriptional induction of UCP-1 expression by



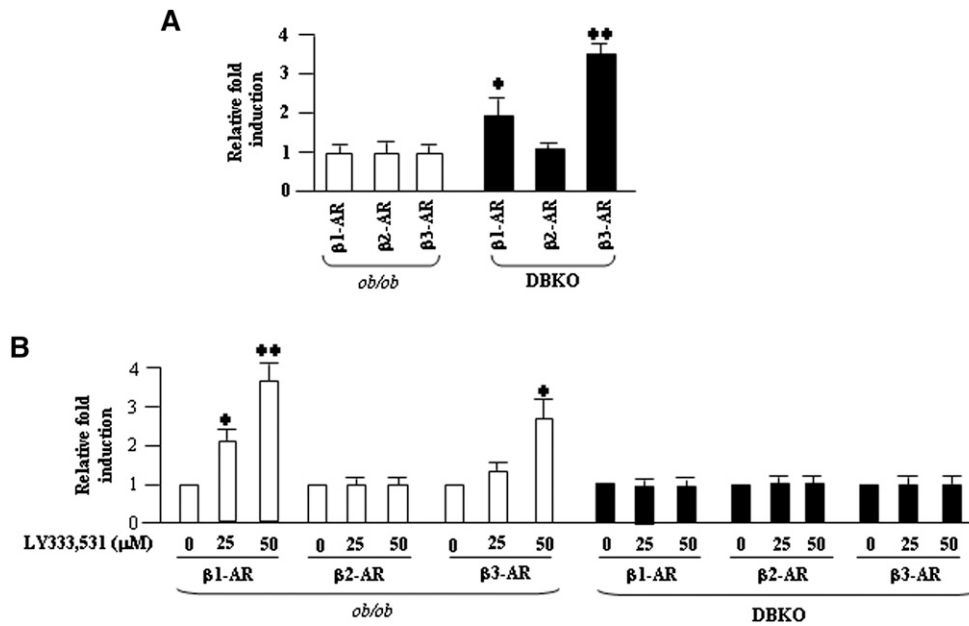


**Fig. 9.** PKC $\beta$ -dependent modulation of  $\beta$ 3-AR signaling in iWAT. A: Expression levels of  $\beta$ -AR subtypes in *ob/ob* and DBKO mice fed HFD for 8 weeks, which were normalized to the expression level in *ob/ob* mice. Levels for each gene in *ob/ob* were assigned a value of 1. B: Adipose tissues explants were isolated from *ob/ob* and DBKO mice. Subsequently, explants were treated with LY333,531 or vehicle. Explants from the same mice were treated with both experimental conditions. Expressions of  $\beta$ -ARs were determined in the explants. Data are represented as means  $\pm$  SD (n = 5 mice per group). \* P < 0.05; \*\*P < 0.01.

PGC-1 $\alpha$ -dependent mechanisms, elevated UCP-1 protein levels in adipose tissues of PKC $\beta$ <sup>-/-</sup> mice could also be due to increased synthesis or stability of UCP-1 protein. One stabilizing influence might be at the level of mitochondria because PKC $\beta$  inhibition has recently been linked to enhanced mitochondrial stability (49). The relevance of this mechanism is underscored by the fact that WAT of PKC $\beta$ <sup>-/-</sup> mice contain more mitochondria and show increased fatty acid oxidation (25). In view of a recent demonstration that PKC $\beta$  mediates insulin-induced hepatic SREBP-1c expression (18), it is likely that reduction in fatty acid synthesis contributes to reduced TG contents of DBKO mice compared with *ob/ob* mice.

Another important aspect of these studies relates to the PKC $\beta$ -dependent, adipocyte-specific  $\beta$ 3-AR expression in fine-tuning the adrenergic signaling in WAT. Results presented here argue strongly in favor of an inverse relationship between PKC $\beta$  and  $\beta$ 3-AR expression. In fact, the proposed relationship is consistent with earlier reports showing that sustained PKC activation suppressed  $\beta$ -ARs expression at the transcriptional level (50–52). It has also been shown that PKC mediates insulin-induced suppression of  $\beta$ 3-AR expression, and this regulation could play a key role in the body's adaptation to antilipolysis, lipogenesis, and thermogenesis that occur during hyperinsulinemic states. Our previous observations that insulin induces PKC $\beta$  expression in white adipocytes and that *ob/ob* WAT has higher PKC $\beta$  expression (26), together with current results showing that DBKO mice have higher  $\beta$ 3-AR expression, strongly support involvement of this isoform in the suppression process and in mediating insulin action on  $\beta$ 3-AR expression in adipocytes. The proposed rela-

tionship may explain significantly reduced  $\beta$ 3-AR mRNA levels in adipose tissues of *ob/ob* mice (53). In fact, other models of congenital obesity, such as *db/db*, *tubby*, *fat*, and Zucker fatty rat, show similar decreases in  $\beta$ 3-AR and  $\beta$ 1-AR expression, the extent of which tends to mirror the severity of obesity (54, 55).

In addition to the potential direct effects of PKC $\beta$  on adipocytes, PKC $\beta$  deficiency may exert other, more global effects that affect overall energy balance. In particular, PKC $\beta$  is expressed in the brain (56), and it may influence PKC $\beta$ -dependent signaling events mediated by leptin at

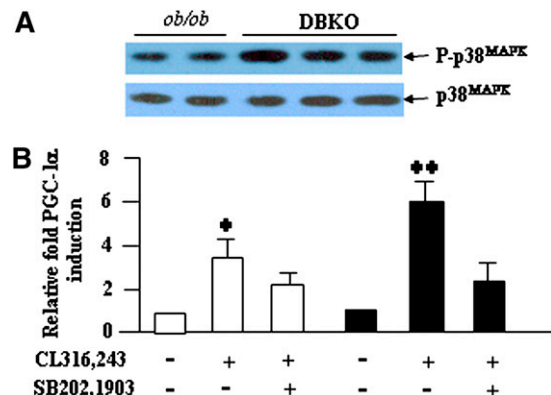



**Fig. 10.**  $\beta$ 3-AR-induced PGC-1 $\alpha$  expression requires p38<sup>MAPK</sup>. A: p38<sup>MAPK</sup> phosphorylation levels in iWAT of both genotypes. B: Inhibition of p38<sup>MAPK</sup> suppressed  $\beta$ 3-AR agonist CL316,243-induced PGC-1 $\alpha$  expression in adipose explants prepared from both genotypes. Levels for untreated controls were assigned a value of 1. Data are represented as means  $\pm$  SD (n = 5 mice per group). \* P < 0.05; \*\*P < 0.01.

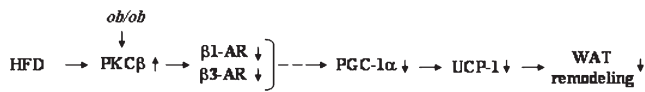


**Fig. 11.** Schematic diagram of the proposed sequence of events whereby PKC $\beta$  deficiency leads to a reduction in metabolic efficiency. Elevated adipose PKC $\beta$  expression in *ob/ob* mice suppresses  $\beta$ -adrenergic signaling and thereby reduces UCP-1 expression in iWAT and prevents WAT catabolic activity.

this site. It is not known whether the metabolic effects of leptin or insulin in the hypothalamus are dependent on the activity of PKC $\beta$ . Our observation that *ob/ob* and DBKO mice consumed similar calories [unlike PKC $\beta$ <sup>-/-</sup> mice, which consume more calories than WT mice (25)] suggests that chronic hypoleptinemia in these animals is responsible for stimulating appetite and argues against an effect of PKC $\beta$  deficiency at the level of the hypothalamus. In addition, our observation that PKC $\beta$  deficiency protected against HFD-induced diabetes even in the *ob/ob* background argues against involvement of leptin-mediated energy expenditure in PKC $\beta$ <sup>-/-</sup> mice.

Beside its role in regulating adiposity, PKC $\beta$  plays an important role in modulating glucose homeostasis. This feature was reflected by lower glucose and insulin levels in DBKO mice compared with those of *ob/ob* mice, suggesting that the metabolic changes induced by PKC $\beta$  deficiency lead to increased insulin sensitivity. Moreover, DBKO mice effectively cleared a glucose bolus that was administered intraperitoneally, whereas *ob/ob* mice stayed hyperglycemic. This phenotype induced by PKC $\beta$  deficiency in *ob/ob* mice supports the hypothesis of lipotoxicity because a decrease in total body lipid content leads to increased insulin sensitivity (57). In this context, it is interesting to note that altering expression of a single gene results in systemic changes in glucose, insulin, and lipid metabolism in a way that protects against the consequences of obesity. We propose a model in which adipose PKC $\beta$  levels determine the metabolic efficiency (Fig. 11). The degree of adrenergic sensitivity, regulated by PKC $\beta$ , could be regarded as a cellular “set point” for metabolism in adipocytes. In this way, pronounced PKC $\beta$  suppression will act as a defense against increasing adipose tissue mass. Based on this model, PKC $\beta$  should be regarded as a candidate target gene for obesity, insulin resistance, and type 2 diabetes. 

We thank Dr. Qinghua Sun for UCP-1 staining.

## REFERENCES

- Zhang, Y., R. Proenca, M. Maffei, M. Barone, L. Leopold, and J. M. Friedman. 1994. Positional cloning of the mouse obese gene and its human homologue. *Nature*. **372**: 425–432.
- Friedman, J. M. 2000. Obesity in the new millennium. *Nature*. **404**: 632–634.
- Ahima, R. S., and J. S. Flier. 2000. Leptin. *Annu. Rev. Physiol.* **62**: 413–437.
- Cohen, B., D. Novick, and M. Rubinstein. 1996. Modulation of insulin activities by leptin. *Science*. **274**: 1185–1188.
- Takekoshi, K., K. Ishii, Y. Kawakami, K. Isobe, T. Nanmoku, and T. Nakai. 2001. Ca(2+) mobilization, tyrosine hydroxylase activity, and signaling mechanisms in cultured porcine adrenal medullary chromaffin cells: effects of leptin. *Endocrinology*. **142**: 290–298.
- Hennige, A. M., N. Stefan, K. Kapp, R. Lehmann, C. Weigert, A. Beck, K. Moeschel, J. Mushack, E. Schleicher, and H. U. Haring. 2006. Leptin down-regulates insulin action through phosphorylation of serine-318 in insulin receptor substrate 1. *FASEB J.* **20**: 1206–1208.
- Kellerer, M., J. Mushack, E. Seffer, H. Mischak, A. Ullrich, and H. U. Haring. 1998. Protein kinase C isoforms alpha, delta and theta require insulin receptor substrate-1 to inhibit the tyrosine kinase activity of the insulin receptor in human kidney embryonic cells (HEK 293 cells). *Diabetologia*. **41**: 833–838.
- Lee, J. W., A. G. Swick, and D. R. Romsos. 2003. Leptin constrains phospholipase C-protein kinase C-induced insulin secretion via a phosphatidylinositol 3-kinase-dependent pathway. *Exp. Biol. Med. (Maywood)* **228**: 175–182.
- Barrenetxe, J., N. Sainz, A. Barber, and M. P. Lostao. 2004. Involvement of PKC and PKA in the inhibitory effect of leptin on intestinal galactose absorption. *Biochem. Biophys. Res. Commun.* **317**: 717–721.
- Payne, G. A., L. Borbouse, S. Kumar, Z. Neeb, M. Alloosh, M. Sturek, and J. D. Tune. 2010. Epicardial perivascular adipose-derived leptin exacerbates coronary endothelial dysfunction in metabolic syndrome via a protein kinase C-beta pathway. *Arterioscler. Thromb. Vasc. Biol.* **30**: 1711–1717.
- Newton, A. C. 2010. Protein kinase C: poised to signal. *Am. J. Physiol. Endocrinol. Metab.* **298**: E395–E402.
- Rosse, C., M. Lynch, S. Kermorgant, A. J. Cameron, K. Boeckeler, and P. J. Parker. 2010. PKC and the control of localized signal dynamics. *Nat. Rev. Mol. Cell Biol.* **11**: 103–112.
- Freeley, M., D. Kelleher, and A. Long. 2011. Regulation of protein kinase C function by phosphorylation on conserved and non-conserved sites. *Cell. Signal.* **23**: 753–762.
- Griner, E. M., and M. G. Kazanietz. 2007. Protein kinase C and other diacylglycerol effectors in cancer. *Nat. Rev. Cancer.* **7**: 281–294.
- Rask-Madsen, C., and G. L. King. 2005. Proatherosclerotic mechanisms involving protein kinase C in diabetes and insulin resistance. *Arterioscler. Thromb. Vasc. Biol.* **25**: 487–496.
- Geraldes, P., and G. L. King. 2010. Activation of protein kinase C isoforms and its impact on diabetic complications. *Circ. Res.* **106**: 1319–1331.
- Patel, N. A., H. S. Apostolatos, K. Mebert, C. E. Chalfant, J. E. Watson, T. S. Pillay, J. Sparks, and D. R. Cooper. 2004. Insulin regulates protein kinase CbetaII alternative splicing in multiple target tissues: development of a hormonally responsive heterologous minigene. *Mol. Endocrinol.* **18**: 899–911.
- Yamamoto, T., K. Watanabe, N. Inoue, Y. Nakagawa, N. Ishigaki, T. Matsuzaka, Y. Takeuchi, K. Kobayashi, S. Yatoh, A. Takahashi, et al. 2010. Protein kinase Cbeta mediates hepatic induction of sterol-regulatory element binding protein-1c by insulin. *J. Lipid Res.* **51**: 1859–1870.
- Formisano, P., F. Oriente, F. Fiory, M. Caruso, C. Miele, M. A. Maitan, F. Andreozzi, G. Vigiotta, G. Condorelli, and F. Beguinot. 2000. Insulin-activated protein kinase Cbeta bypasses Ras and stimulates mitogen-activated protein kinase activity and cell proliferation in muscle cells. *Mol. Cell. Biol.* **20**: 6323–6333.
- Aguirre, V., E. D. Werner, J. Giraud, Y. H. Lee, S. E. Shoelson, and M. F. White. 2002. Phosphorylation of Ser307 in insulin receptor substrate-1 blocks interactions with the insulin receptor and inhibits insulin action. *J. Biol. Chem.* **277**: 1531–1537.
- Ishizuka, T., K. Kajita, Y. Natsume, Y. Kawai, Y. Kanoh, A. Miura, M. Ishizawa, Y. Uno, H. Morita, and K. Yasuda. 2004. Protein kinase C (PKC) beta modulates serine phosphorylation of insulin receptor substrate-1 (IRS-1)—effect of overexpression of PKCbeta on insulin signal transduction. *Endocr. Res.* **30**: 287–299.
- Osterhoff, M. A., S. Heuer, M. Pfeiffer, J. Tasic, S. Kaiser, F. Isken, J. Spranger, M. O. Weickert, M. Mohlig, and A. F. Pfeiffer. 2008. Identification of a functional protein kinase Cbeta promoter polymorphism in humans related to insulin resistance. *Mol. Genet. Metab.* **93**: 210–215.
- Biden, T. J., C. Schmitz-Peiffer, J. G. Burchfield, E. Gurisik, J. Cantley, C. J. Mitchell, and L. Carpenter. 2008. The diverse roles of protein kinase C in pancreatic  $\beta$ -cell function. *Biochem. Soc. Trans.* **36**: 916–919.
- Pinton, P., T. Tsuboi, E. K. Ainscow, T. Pozzan, R. Rizzuto, and G. A. Rutter. 2002. Dynamics of glucose-induced membrane recruitment of protein kinase C  $\beta$ II in living pancreatic islets  $\beta$ -cells. *J. Biol. Chem.* **277**: 37702–37710.
- Huang, W., R. Bansode, M. Mehta, and K. D. Mehta. 2009. Loss of protein kinase Cbeta function protects mice against diet-induced obesity and development of hepatic steatosis and insulin resistance. *Hepatology*. **49**: 1525–1536.

26. Bansode, R. R., W. Huang, S. K. Roy, M. Mehta, and K. D. Mehta. 2008. Protein kinase C deficiency increases fatty acid oxidation and reduces fat storage. *J. Biol. Chem.* **283**: 231–236.
27. Butler, A. A., and L. P. Kozak. 2010. A recurring problem with the analysis of energy expenditure in genetic models expressing lean and obese phenotypes. *Diabetes*. **59**: 323–329.
28. Kaiyala, K. J., G. J. Morton, B. G. Leroux, K. Ogimoto, B. Wisse, and M. W. Schwartz. 2010. Identification of body fat mass as a major determinant of metabolic rate in mice. *Diabetes*. **59**: 1657–1666.
29. Rothwell, N. J., and M. J. Stock. 1979. A role for brown adipose tissue in diet-induced thermogenesis. *Nature*. **281**: 31–35.
30. Brooks, S. L., N. J. Rothwell, M. J. Stock, A. E. Goodbody, and P. Trayhurn. 1980. Increased proton conductance pathway in brown adipose tissue mitochondria of rats exhibiting diet-induced thermogenesis. *Nature*. **286**: 274–276.
31. Glick, Z., R. J. Teague, and G. A. Bray. 1981. Brown adipose tissue: thermic response increased by a single low protein, high carbohydrate meal. *Science*. **213**: 1125–1127.
32. Jung, R. T., P. S. Shetty, W. P. James, M. A. Barrand, and B. A. Callingham. 1979. Reduced thermogenesis in obesity. *Nature*. **279**: 322–323.
33. Bouillaud, F., D. Ricquier, G. Mory, and J. Thibault. 1984. Increased level of mRNA for the uncoupling protein in brown adipose tissue of rats during thermogenesis induced by cold exposure or norepinephrine infusion. *J. Biol. Chem.* **259**: 11583–11586.
34. Himms-Hagen, J. 1985. Brown adipose tissue metabolism and thermogenesis. *Annu. Rev. Nutr.* **5**: 69–94.
35. Granneman, J. G., P. Li, Z. Zhu, and Y. Lu. 2005. Metabolic and cellular plasticity in white adipose tissue I: effects of  $\beta$ 3-adrenergic receptor activation. *Am. J. Physiol. Endocrinol. Metab.* **289**: E608–E616.
36. Guerra, C., R. A. Koza, H. Yamashita, K. Walsh, and L. P. Kozak. 1998. Emergence of brown adipocytes in white fat in mice is under genetic control: Effects on body weight and adiposity. *J. Clin. Invest.* **102**: 412–420.
37. Himms-Hagen, J., J. Cui, E. Danforth, D. J. Taatjes, S. S. Lang, B. L. Waters, and T. H. Claus. 1994. Effect of CL-316,243, a thermogenic  $\beta$ 3-agonist, on energy balance and brown and white adipose tissues in rats. *Am. J. Physiol. Regul. Integr. Comp. Physiol.* **266**: R1371–R1382.
38. Himms-Hagen, J., A. Melnyk, M. C. Zingaretti, E. Ceresi, G. Barbatelli, and T. H. Cinti. 2000. Multilocular fat cells in WAT of CL-316243-treated rats derive directly from white adipocytes. *Am. J. Physiol. Cell Physiol.* **279**: C670–C681.
39. Cederberg, A., L. M. Gronning, B. Ahren, K. Tasken, P. Carlsson, and S. Enerback. 2001. FOXC2 is a winged helix gene that counteracts obesity, hypertriglyceridemia, and diet-induced insulin resistance. *Cell*. **106**: 563–573.
40. Cummings, D. E., E. P. Brandon, J. V. Planas, K. Motamed, R. L. Idzarda, and G. S. McKnight. 1996. Genetically lean mice result from targeted disruption of the RII beta subunit of protein kinase A. *Nature*. **382**: 622–626.
41. Kopecky, J., G. Clarke, S. Enerback, B. Spiegelman, and L. P. Kozak. 1995. Expression of the mitochondrial uncoupling protein gene from the aP2 gene promoter prevents genetic obesity. *J. Clin. Invest.* **96**: 2914–2923.
42. Kopecky, J., Z. Hondy, M. Rossmey, I. Syrový, and L. P. Kozak. 1996. Reduction of dietary obesity in aP2-UCP transgenic mice: physiology and adipose tissue distribution. *Am. J. Physiol.* **270**: E768–E775.
43. Zhou, Z., T. S. Yon, Z. Chen, K. Guo, C. P. Ng, S. Ponniah, S. C. Lin, W. Hong, and P. Li. 2003. Cidea-deficient mice have lean phenotype and are resistant to obesity. *Nat. Genet.* **35**: 49–56.
44. Lin, J., C. Handschin, and B. M. Spiegelman. 2005. Metabolic control through the PGC-1 family of transcription coactivators. *Cell Metab.* **1**: 361–370.
45. Nemoto, S., M. M. Fergusson, and T. Finkel. 2005. SIRT1 functionally interacts with the metabolic regulator and transcriptional coactivator PGC-1[alpha]. *J. Biol. Chem.* **280**: 16456–16460.
46. Chen, W., Q. Yang, and R. G. Roeder. 2009. Dynamic interactions and cooperative functions of PGC-1alpha and MED1 in TRalpha-mediated activation of the brown-fat-specific UCP-1 gene. *Mol. Cell.* **35**: 755–768.
47. Shi, T., F. Wang, E. Stieren, and Q. Tong. 2005. SIRT3, a mitochondrial sirtuin deacetylase, regulates mitochondrial function and thermogenesis in brown adipocytes. *J. Biol. Chem.* **280**: 13560–13567.
48. Tiraby, W., G. Tavernier, C. Lefort, D. Larrouy, F. Bouillaud, D. Ricquier, and D. Langin. 2003. Acquisition of brown fat cell features by human white adipocytes. *J. Biol. Chem.* **278**: 33370–33376.
49. Pinton, P., A. Rimessi, S. Marchi, F. Orsini, E. Migliaccio, M. Giorgio, C. Contursi, S. Minucci, F. Mantovani, M. R. Wieckowski, et al. 2007. Protein kinase C beta and prolyl isomerase 1 regulate mitochondrial effects of the life-span determinant p66Shc. *Science*. **315**: 659–663.
50. Li, Z., V. A. Vaidya, J. D. Alvaro, P. A. Iredale, R. Hsu, G. Hoffman, L. Fitzgerald, P. K. Curran, C. A. Machida, P. H. Fishman, et al. 1998. Protein kinase C-mediated down-regulation of beta1-adrenergic receptor gene expression in rat C6 glioma cells. *Mol. Pharmacol.* **54**: 14–21.
51. Fève, B., K. Elhadri, A. Quignard-Boulangé, and J. Pairault. 1994. Transcriptional down-regulation by insulin of the beta 3-adrenergic receptor expression in 3T3-F442A adipocytes: a mechanism for repressing the cAMP signaling pathway. *Proc. Natl. Acad. Sci. USA*. **91**: 5677–5681.
52. Fève, B., F. Pietri-Rouxel, K. Hadri, M. F. Drumare, and A. D. Strosberg. 1995. Long term phorbol ester treatment down-regulates the beta 3-adrenergic receptor in 3T3-F442A adipocytes. *J. Biol. Chem.* **270**: 10952–10959.
53. Collins, S., K. W. Daniel, E. M. Rohlf, V. Ramkumar, I. L. Taylor, and T. W. Gettys. 1994. Impaired expression and functional activity of the beta 3- and beta 1-adrenergic receptors in adipose tissue of congenitally obese (C57BL/6j ob/ob) mice. *Mol. Endocrinol.* **8**: 518–527.
54. Muzzin, P., J. P. Revelli, F. Kuhne, J. D. Gocayne, W. R. McCombie, J. C. Venter, J. P. Giacobino, and C. M. Fraser. 1991. An adipose tissue-specific beta-adrenergic receptor. Molecular cloning and down-regulation in obesity. *J. Biol. Chem.* **266**: 24053–24058.
55. Collins, S., K. W. Daniel, and E. M. Rohlf. 1999. Depressed expression of adipocyte beta-adrenergic receptors is a common feature of congenital and diet-induced obesity in rodents. *Int. J. Obes. Relat. Metab. Disord.* **23**: 669–677.
56. Saito, N., A. Kose, A. Ito, K. Hosoda, M. Mori, M. Hirata, K. Ogita, U. Kikkawa, Y. Ono, and K. Igarashi. 1989. Immunocytochemical localization of beta II subspecies of protein kinase C in rat brain. *Proc. Natl. Acad. Sci. USA*. **86**: 3409–3413.
57. Unger, R. H., and L. Orci. 2000. Lipotoxic disease of nonadipose tissues in obesity. *Int. J. Obes. Relat. Metab. Disord.* **24**: 28–32.